

<https://doi.org/10.1038/s41523-024-00697-5>

Clinical and immune responses to neoadjuvant fulvestrant with or without enzalutamide in ER⁺/Her2[–] breast cancer

Check for updates

Anthony D. Elias¹, Alyse W. Staley^{2,3}, Monica Fornier⁴, Gregory A. Vidal⁵, Vida Alami³, Sharon Sams⁶, Nicole S. Spoelstra⁶, Andrew Goodspeed^{7,8}, Peter Kabos¹, Jennifer R. Diamond¹, Elena Shagisultanova¹, Rosa I. Gallagher⁹, Julia D. Wulfkuhle⁹, Emanuel F. Petricoin⁹, Kathryn L. Zolman⁶, Tessa McSpadden¹⁰, Kimberly R. Jordan¹¹, Jill E. Slansky¹¹, Virginia F. Borges¹, Dexiang Gao^{2,3} & Jennifer K. Richer⁶✉

Most ER⁺ breast cancers (BC) express androgen receptors (AR). This randomized phase II trial of 4 months of neoadjuvant fulvestrant (Fulv) alone or with enzalutamide (Combo) assessed whether adding AR blockade to Fulv would limit residual tumor at the time of surgery, as measured by modified preoperative endocrine predictive index (PEPI) score. Eligible patients were women with ER⁺/HER2[–] primary BC cT2 or greater. Stratification factors were clinical node and T-stage. Fresh tumor biopsies were required at study entry, after 4 weeks on therapy (W5), and at surgery. Laboratory analyses on tumors included immunohistochemistry (IHC) for ER/PR/AR/GR and Ki67 protein, evaluation of gene expression, multiplex for myeloid lineage immune cells, reverse-phase protein array, and plasma metabolomic analyses. Of 69 consented patients, 59 were evaluable. Toxicity was as expected with endocrine therapy. Combo achieved PEPI = 0 more frequently (24%: 8/33) than Fulv (8%: 2/26). Ki67 was ≤10% across arms by W5 in 76% of tumors. Activation of mTOR pathway proteins was elevated in tumors with poor Ki67 response. Tumors in both arms showed decreased estrogen-regulated and cell division gene sets, while Combo arm tumors uniquely exhibited enrichment of immune activation gene sets, including interferon gamma, complement, inflammation, antigen processing, and B and T cell activation. Multiplex IHC showed significantly reduced tumor-associated macrophages and CD14⁺/HLADR[–]/CD68[–] MDSCs in Combo tumors at W5. In summary, Combo tumors showed a higher PEPI = 0 response, Ki67 response, and more activated tumor immune microenvironment than Fulv. The odds of response were 4.6-fold higher for patients with ILC versus IDC. (Trial registration: This trial is registered at Clinicaltrials.gov (<https://www.clinicaltrials.gov/study/NCT02955394?id=16-1042&rank=1>). The trial registration number is NCT02955394. The full trial protocol is available under Study Details at the Clinicaltrials.gov link provided).

Neoadjuvant therapy is often administered to more locally advanced breast cancer (BC) to facilitate surgery, downstage the tumor, and evaluate the efficacy of systemic therapy. Although chemotherapy is usually the modality of choice, it is increasingly recognized that more indolent, estrogen-driven BC may not benefit significantly from chemotherapy, and pre-operative endocrine therapy may be administered, with a reassessment of therapeutic options in the adjuvant setting based on surgical results and

clinical risk. The optimal choice for neoadjuvant endocrine therapy is not yet fully established.

While the majority (over 90%) of all estrogen receptor-positive (ER⁺) BCs express androgen receptor (AR) protein^{1,2}, its role remains controversial. In the presence of estrogen, androgens tend to suppress ER-mediated proliferation in preclinical models. In contrast, when ER signaling is absent (in postmenopausal women, especially those with BC on aromatase inhibitors

(AIs) or tumors where ER is low), androgens stimulate proliferation and enhance survival of tumor cells while anti-androgens reduce proliferation. Although AR is associated with more indolent luminal tumors, high AR protein expression relative to ER is associated with resistance to tamoxifen and AI therapy as supported by both clinical and preclinical data³⁻⁷.

We hypothesized that the anti-androgen agent enzalutamide (E), when combined with the ER degrader fulvestrant (Fulv), would enhance anti-proliferative activity. Fulv was selected as the ER-targeting agent for this trial because it is at least equally as effective against ER+ BC as aromatase inhibitors and has little pharmacologic interaction with E. The safety of Fulv plus E was established in a phase I trial. E is a powerful CYP3A4 inducer and reduced the AUC of exemestane by 50% and anastrozole by 88%, but the AUC of fulvestrant was not affected⁸. Subsequently, a non-randomized phase II trial of Fulv plus E conducted in patients with heavily pre-treated metastatic ER+HER2- BC not selected for AR expression, achieved a clinical benefit rate (CBR) at 24 weeks of 25%⁹. In contrast, a selective AR modulator (SARM), enobosarm, was recently evaluated as a single agent in a group of endocrine-sensitive patients, of which 20% had untreated de novo metastatic disease. CBR for this selected group of patients was 31% study-wide; however, 25% of the intent-to-treat patients were excluded from the CBR calculation due to lack of confirmed ≥10% AR+staining¹⁰. Further, 36% of patients had bone only disease (not always evaluable and typically not measurable), and 16% of patients had G3 toxicity related to drug, including two with G3 “tumor flare”¹⁰.

Here, we report the results of a randomized phase II trial with Fulv alone or in combination with E (Combo) given preoperatively for 4 months to patients with primary, untreated BC. The primary objective was to compare the preoperative endocrine predictive index (PEPI) score in the two arms. Secondary clinical objectives were to further confirm the safety profile

of this combination and evaluate Ki67 change. Serial biopsies and plasma were obtained pretreatment as a baseline (BL) measurement, at the end of the fourth week of treatment (W5), and at the time of surgery, to evaluate the effects of treatment on tumor and its relationship to clinical outcomes.

Results

Patient characteristics and clinical outcomes

A total of 69 patients consented and were screened, of whom 59 were evaluable: 33 on Combo and 26 on Fulv (Fig. 1B CONSORT diagram). Upon completion of the Simon stage I portion of the experimental arm, 4/22 patients (18%) had achieved PEPI = 0, so the second stage then completed accrual. Demographics are depicted in Table 1. Of the 33 patients treated on the Combo arm, the median age was 63. At BL, 21% had T3/T4 tumors, 91% were ER+/PR+, median AR expression was 80%, and median Ki67 was 15%. Of the 26 patients treated on the Fulv arm, the median age was 61, 19% had T3/T4 tumors, 96% were ER+/PR+, median AR expression was 85%, and median Ki67 was 10%. Across both arms, surgery was completed in 56/59 patients (95%), with endocrine therapy alone. Three received chemotherapy prior to surgery, and these were designated as PEPI > 0. Overall, PEPI = 0 was achieved in 10/59 (17%). Importantly, PEPI = 0 was achieved more frequently on the Combo arm (8/33, 24%) than the Fulv arm (2/26, 8%) (p = 0.16) (Table 2). However, this did not meet pre-specified significance (0.08).

Toxicity was as expected with endocrine therapy (Table 3). Mild cognitive disturbance was noted primarily (described as “feeling woozy,” “a bit out of it,” and “trouble concentrating”) in patients receiving E (the Combo arm). These appeared fully reversible upon completing E. Mild nausea, diarrhea, sleep disturbance, and fatigue were also more common in the Combo arm.

Fig. 1 | Flow of study. a Study schema. **b** CONSORT diagram flow chart. *Three were ineligible, four withdrew for surgery first. †Not treated (surgery first). **Treated for 4 weeks until W5 biopsy demonstrated Her2 amplification and withdrawn by MD; inevaluable.

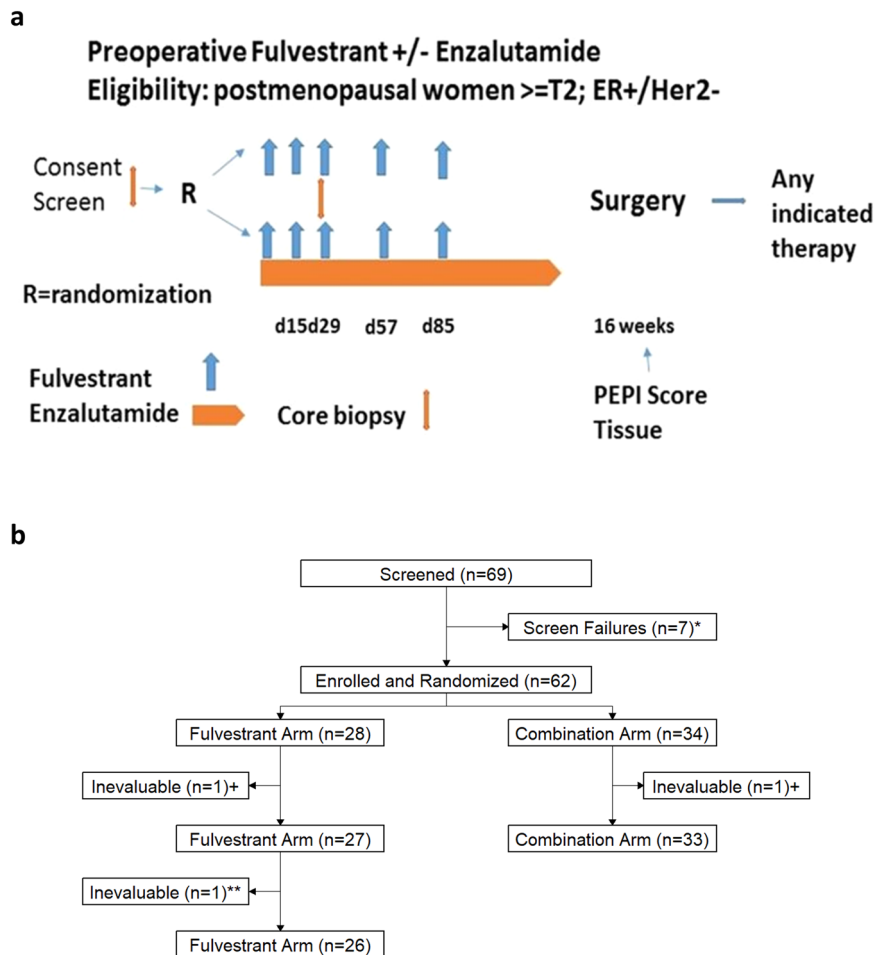


Table 1 | Baseline patient characteristics

	Combo arm (N = 33)	Fulv arm (N = 26)	Total (N = 59)	PEPI = 0 (N = 10)
Age at consent (years)				
Median (range)	63 (41, 78)	61 (32, 83)	63 (32, 83)	66 (49, 76)
ECOG PS				
Median (range)	0 (0, 1)	0 (0, 2)	0 (0, 2)	0 (0, 1)
T stage				
T2	26 (78.8%)	21 (80.8%)	47 (79.7%)	9 (90.0%)
T3	6 (18.2%)	5 (19.2%)	11 (18.6%)	1 (10.0%)
T4	1 (3.0%)	0 (0.0%)	1 (1.7%)	0 (0.0%)
N stage				
NX	1 (3.0%)	0 (0.0%)	1 (1.7%)	0 (0.0%)
N0	14 (42.4%)	13 (50%)	27 (45.8%)	10 (100.0%)
N1	17 (51.5%)	13 (50%)	30 (50.8%)	0 (0.0%)
N2	1 (3.0%)	0 (0.0%)	0 (0.0%)	0 (0.0%)
ER/PR expression positive^a				
ER+ & PR-	3 (9.1%)	1 (3.8%)	4 (6.8)	2 (20.0%)
ER+ & PR+	30 (90.9%)	25 (96.2%)	55 (93.2%)	8 (80.0%)
% AR expression positive^a				
N	27	22	49	9
Median (range)	80 (10, 100)	85 (10, 100)	80 (10, 100)	90 (10, 100)
Ki67 (%)				
N	29	21	50	10
Median (range)	15 (1, 80)	10 (1, 60)	12 (1, 80)	5 (1, 15)
Histology				
IDC	25 (75.8%)	20 (76.9%)	45 (76.3%)	5 (50.0%)
ILC	5 (15.2%)	6 (23.1%)	11 (18.6%)	4 (40.0%)
Other	3 (9.1%)	0 (0.0%)	3 (5.1%)	1 (10.0%)

N is presented for variables with less than 59 observations.

^aLab data were used to calculate AR, ER, and PR % Positive. ER and PR % Positive were replaced with clinical data when lab data were unavailable.

Demographic and clinical risk factors of progression

Univariate associations between PEPI score and clinical variables showed that lower BL and W5 Ki67 were associated with greater odds of PEPI = 0 score. The odds of response (PEPI = 0) decreased 9.9% (95% CI: 2.3–20.6, $p = 0.004$) per percentage point higher BL Ki67 and 38.1% (95% CI: 5.3–71.1, $p = 0.005$) per percentage point higher W5 Ki67. Only one patient had a T3 tumor that achieved PEPI = 0, and this was on the Combo arm. None of the PEPI = 0 patients were node-positive (Table 1). Interestingly, the odds of response were 4.6-fold higher (95% CI: 0.9–22 times, $p = 0.06$) for patients with ILC versus those with IDC. Age at consent ($p = 0.13$), ER IHC ($p = 0.47$ at BL, $p = 0.30$ at W5, $p = 0.34$ at Surgery), and AR IHC ($p = 0.96$ at BL, $p = 0.71$ at W5, $p = 0.34$ at Surgery) were not significantly associated with PEPI score (Table 4).

Serial tissue studies

The steroid receptors ER, PR, AR, glucocorticoid receptor (GR), Ki67; and cleaved caspase 3 were quantified by immunohistochemistry (IHC) across arms in tumor tissue at BL, W5, and time of surgery (Fig. 2, Table 2, Supplementary Fig. 1). ER (Combo W5 $p < 0.001$, Combo surgery $p < 0.001$, Fulv W5 $p < 0.001$, Fulv surgery $p = 0.012$) and PR (Combo W5 $p < 0.001$, Combo surgery $p = 0.002$, Fulv W5 $p = 0.001$,

Table 2 | Surgical and Ki67 results

	Combo arm (N = 33)	Fulv arm (N = 26)	Total (N = 59)
Surgery^a			
No	2 (6.1%)	1 (3.8%)	3 (5.1%)
Yes	31 (93.9%)	25 (96.2%)	56 (94.9%)
PEPI Score			
>0	25 (75.8%)	24 (92.3%)	49 (83.1%)
0	8 (24.2%)	2 (7.7%)	10 (16.9%)
Ki67 at W5^b			
N	26	24	50
≤10%	18 (69.2%)	20 (83.3%)	38 (76.0%)
Ki67 at surgery^b			
N	26	22	48
≤10%	19 (73.1%)	17 (77.3%)	36 (75.0%)
Change in Ki67 BL – W5			
N	26	22	48
High BL, High W5	8 (30.8%)	4 (18.2%)	12 (25.0%)
High BL, Low W5 ^c	11 (42.3%)	9 (40.9%)	20 (41.7%)
Low BL, Low W5	7 (26.9%)	9 (40.9%)	16 (33.3%)
Change in Ki67 BL – surgery			
N	25	20	45
High BL, high surgery	7 (28.0%)	4 (20.0%)	11 (24.4%)
High BL, low surgery	11 (44.0%)	7 (35.0%)	18 (40.0%)
Low BL, high surgery	0 (0.0%)	1 (5.0%)	1 (2.2%)
Low BL, low surgery	7 (28.0%)	8 (40.0%)	15 (33.3%)

N is provided for variables with less than 59 variables, and the percentage shown is out of the non-missing total.

^a“Yes” indicates patients who had surgery during the study, and “No” indicates patients who did not have surgery during the study. Three patients did not have surgery: one insurance-related, and two received additional therapy prior to surgery due to the physician’s decision.

^b“≤10%” indicates patients who had low Ki67 (≤10%) as measured by IHC at each time point. High Ki67 is defined as >10%.

^cThe high BL, low W5 group are designated as responders by Ki67.

Fulv surgery $p = 0.001$) were significantly decreased in both arms at both W5 and time of surgery. AR ($p = 0.021$) and GR ($p = 0.048$) decreased significantly only in the Combo arm at the time of surgery. Among patients with complete Ki67 data, 11/25 (44%) in the Combo arm and 7/20 (35%) in the Fulv arm had BL Ki67 >10%, which decreased to ≤10% at the time of surgery (Table 2). Ten patients (4 on Combo and 6 in Fulv) had a delay in surgery; however, the delayed timing of surgery did not significantly affect Ki67 or AR between W5 and surgery in these patients. In the Combo arm, no tumors had increased Ki67 between BL and time of surgery, but an increase in Ki67 was observed in 3 patients on Fulv only (Fig. 2).

Reverse-phase protein array

Reverse-phase protein array (RPPA) data measured differences in phosphoprotein abundance across various definitions of response. Figure 3A depicts dumbbell plots of significant differences ($p < 0.1$) in phosphoprotein expression at BL in tumors destined to achieve PEPI = 0 versus PEPI > 0. Cell cycle proteins were significantly lower at BL in tumors destined to have a PEPI = 0 response, as were stress response (pHSP90), DNA damage repair, and growth/survival/ and

Table 3 | Summary of treatment-related adverse events (trAEs)

	Combo arm (N = 33)	Fulv arm (N = 26)	Total (N = 59)
Patients with any trAE(s)	28 (84.8%)	20 (77%)	48 (81.4%)
Patients with any Grade 3/4 trAE(s)	1 (3%) ^a	1 (3.8%) ^b	2 (3.4%)
Grade 1/2 trAEs ≥ 10%^c			
Gastrointestinal	18 (54.5%)	8 (30.8%)	26 (44.1%)
Nausea	13 (39.4%)	3 (11.5%)	16 (27.1%)
Diarrhea	6 (18.2%)	1 (3.8%)	7 (11.9%)
Weight loss	3 (9.1%)	1 (3.8%)	4 (6.8%)
Constipation	2 (6.1%)	3 (11.5%)	5 (8.5%)
General	17 (51.5%)	8 (30.8%)	25 (42.4%)
Fatigue	16 (48.5%)	7 (26.9%)	23 (39%)
Endocrine	15 (45.5%)	8 (30.8%)	23 (39%)
Hot flashes	15 (45.5%)	8 (30.8%)	23 (39%)
CNS	16 (48.5%)	5 (19.2%)	21 (35.6%)
Headache	11 (33.3%)	2 (7.7%)	13 (22%)
Cognitive disturbance	6 (18.2%)	1 (3.8%)	7 (11.9%)
Dizziness	4 (12.1%)	0	4 (6.8%)
Musculoskeletal	11 (33.3%)	7 (26.9%)	18 (30.5%)
Arthralgia	5 (15.2%)	4 (15.4%)	9 (15.3%)
Myalgia	7 (21.2%)	2 (7.7%)	9 (15.3%)
Psychiatric	12 (36.4%)	1 (3.8%)	13 (22%)
Insomnia	7 (21.2%)	0	7 (11.9%)
Skin	5 (15.2%)	1 (3.8%)	6 (10.2%)
Genitourinary	4 (12.1%)	0	4 (6.8%)

The table includes trAEs determined to be probably or possibly related to treatment. Percentages are out of column totals. Category counts include infrequent trAEs not listed in the table.

^aMyocardial infarction, grade 4.

^bALT increase, grade 3.

^cOccurred in ≥10% of patients in total or in at least one arm.

metabolism proteins. Additionally, total AR, pS81, and p650AR, as well as total PD-L1, were lower in PEPI = 0. Three RTKs were also lower at BL in tumors that would achieve PEPI = 0. pHER3 and pHER2 were higher at BL in tumors that achieved PEPI = 0.

Change with treatment (from BL to W5) was also compared by PEPI response (Fig. 3B). Tumors that achieved PEPI = 0 showed decreased phosphoproteins in the cell cycle, cellular stress, growth/survival/metabolism, HER family, and RTKs (except for PRAS40 T246) by W5 of treatment. Importantly, total AR (as detected by two different antibodies) was significantly reduced by W5 in tumors achieving PEPI = 0 (8 out of 10 of which were in the Combo arm). Significant protein changes with $p < 0.2$ are listed in Supplementary Figs. 2–4.

Similarly, Fig. 4A depicts significant differences ($p < 0.1$) in phosphoprotein levels at BL in tumors destined to respond by reduced Ki67 (as measured by IHC) (Ki67 high BL/low W5) were compared to non-responders (Ki67 high BL/high W5), where high Ki67 was defined as >10%, and low Ki67 was defined as ≤10%. Cell cycle proteins, including RPPA Ki67 itself, HSP90aT5/T7, DNA damage repair proteins, mTOR activation indicators, and Nfkbp65S536, were lower at BL in Ki67 responders. In tumors that did not respond (Ki67 high BL/high W5), Y1248HER2 and pS650AR were low at BL.

Ki67 response groups were also compared post-treatment (W5–BL) (Fig. 4B). As expected, Ki67 detected by RPPA decreased in tumors that showed decreased Ki67 quantified by IHC. Activated MEK, mTOR, and other pro-survival and metabolism proteins also decreased in Ki67-responsive tumors (Ki67 high BL/low W5). pHER2, AR total, and p

Table 4 | Univariate associations with PEPI Score (PEPI = 0, PEPI > 0)

Univariate predictors	N	OR	95% CI	p-value
Age at consent (years)	59	1.05	0.99, 1.13	0.13
Lab AR (%)				
Baseline Lab AR (%)	55	1	0.98, 1.03	0.96
Week 5 Lab AR (%)	51	1	0.97, 1.02	0.71
Surgery Lab AR (%)	50	0.99	0.97, 1.01	0.34
Lab ER (%)				
Baseline Lab ER (%)	55	0.99	0.97, 1.01	0.47
Week 5 Lab ER (%)	51	0.99	0.96, 1.01	0.3
Surgery Lab ER (%) ^a	50	0.99	0.97, 1.01	0.34
Ki67 (%)				
Baseline Ki67 (%)	50	0.9	0.79, 0.98	0.004
Week 5 Ki67 (%)	49	0.62	0.29, 0.95	0.005
Histology	56			0.059
Invasive ductal carcinoma (IDC)	45	–	–	
Invasive lobular carcinoma (ILC)	11	4.57	0.94, 21.97	

Univariate logistic regression models with PEPI score (PEPI = 0 vs reference: PEPI > 1) as the outcome are presented with profile likelihood CIs and likelihood ratio test (LRT) p-values. Odds ratios above one indicate increases in the odds of response (PEPI = 0), and odds ratios below one indicate decreases in the odds of response.

OR odds ratio, CI confidence interval.

^aWhile Lab ER at the time of surgery was included in the PEPI score, other components of PEPI score dictated whether patients were 0 or non-zero.

S650AR also decreased with treatment in responding tumors. IGF1R Y1135/1136 and/or insulin receptor Y1150/51 were significantly increased ($p < 0.1$) with treatment in non-responsive tumors, while pCHK1 and pAXL decreased. Significant protein changes with $p < 0.2$ are listed in Supplementary Figs. 5, 6.

Finally, since the odds of PEPI = 0 response were 4.6-fold (95% CI: 0.9–22) higher for patients with ILC compared to those with IDC, we examined the phosphoproteins in these two histologic groups at BL and the change with treatment. BL Cyclin D1, S6RP, HIF-1 alpha, and ATP citrate lyase were significantly lower in ILC than in IDC. CHK1 and ALK were higher (Supplementary Fig. 7A and Supplementary Fig. 8). Interestingly, on average, both AR and phosphoS650 AR decreased more from BL to W5 in ILC compared to IDC. As would be expected with the higher odds of response in ILC as measured by PEPI score, multiple cell cycle proteins decreased more with treatment in ILC, as did most growth/survival/metabolism proteins, except for PRAS40 and PLCgamma1, which increased with treatment in ILC (Supplementary Fig. 7B and Supplementary Fig. 9).

Metabolomics from patient plasma

Plasma metabolic analytes demonstrated a significant change with treatment (W5–BL) across PEPI response groups (PEPI = 0, PEPI > 0), independent of arm (Fig. 5A). In general, metabolites associated with fatty acid synthesis, such as L-carnitine, acyl-C5:1, sphingosine 1-phosphate, dodecanedioic acid, and lactate, were lower at BL in tumors that ultimately achieved PEPI = 0 than in PEPI > 0 tumors. Additionally, 2-oxoglutarate, octanoic acid, 2',3'-cyclic CMP, mannitol, and sphinganine 1-phosphate increased in these tumors. Figure 5B depicts analytes that significantly changed with treatment across arms. The Combo arm had a greater effect than Fulv alone in reducing multiple amino acids, fatty acids, glycerophospholipid synthesis, indoles, succinate, and the urea cycle by W5, whereas GSH homeostasis and bilirubin increased. Significant metabolite changes with $p < 0.2$ are listed in Supplementary Figs. 10, 11.

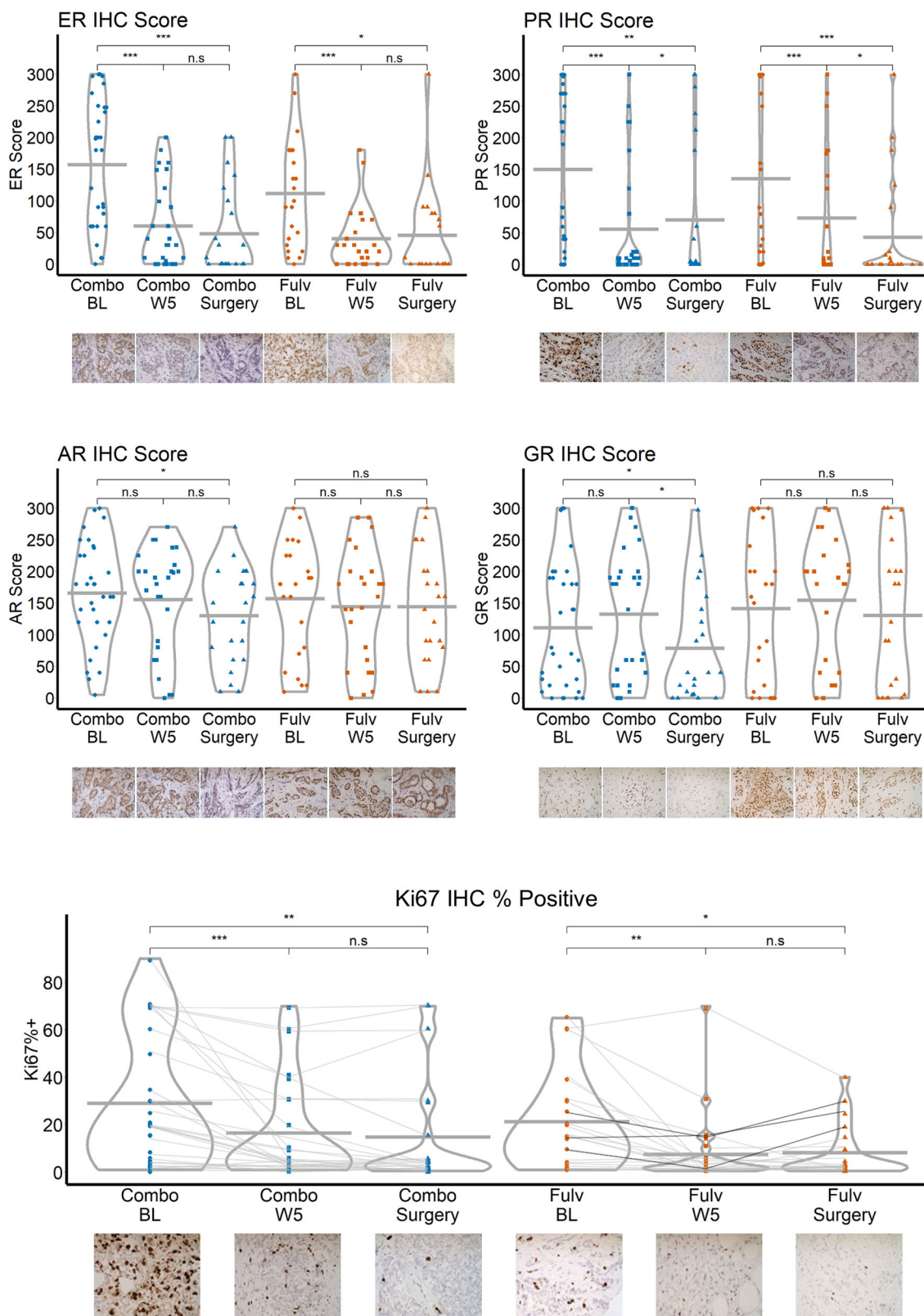
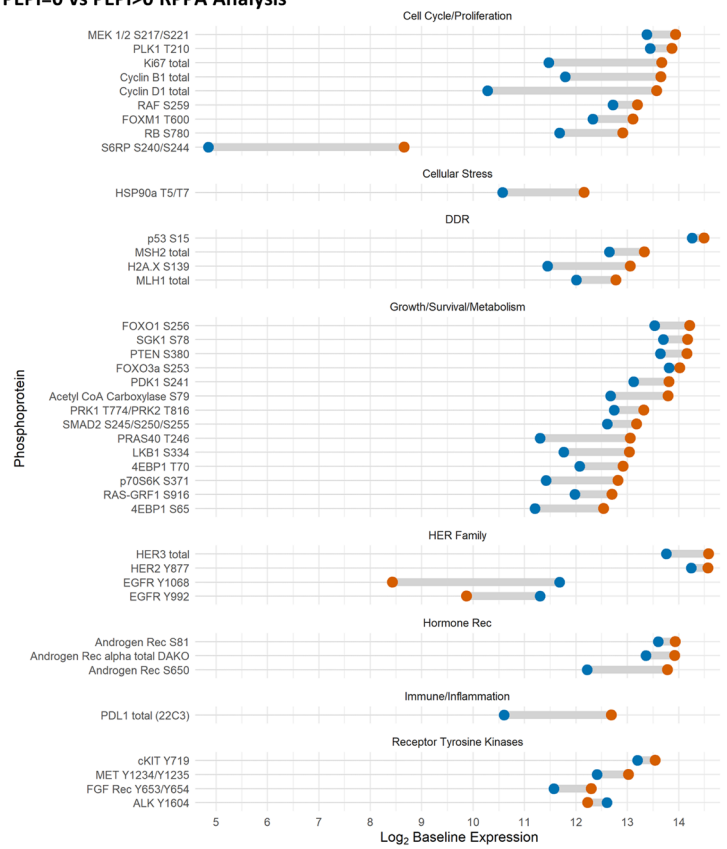


Fig. 2 | Immunohistochemistry (IHC) in serial biopsies by treatment arm and time. Points represent individual observations and horizontal lines indicate the mean in each group. *T*-tests were used to compare the Combo and Fulv arms for each outcome and time point. Paired *t*-tests were used to evaluate within-group

changes over time. “n.s.,” “*,” “**,” and “***” indicate non-significance ($p > 0.05$), $p < 0.05$, $p < 0.01$, and $p < 0.001$, respectively. Images of one patient’s paired samples over time are shown for each protein under the *x*-axis as an example. Data points in the Ki67 plot are vertically jittered up to one unit. Magnification = 400 \times .

Fig. 3 | RPPA by PEPI score. Reverse-phase phosphoprotein analysis (RPPA) was performed on laser-captured, fresh frozen tumor that was split into two groups for comparison: PEPI = 0 (blue, $N = 9$) tumors that responded to treatment, and PEPI > 0 (orange, $N = 45$) tumors that did not. Tumors came from patients in both arms. Presented phosphoproteins were significantly ($p < 0.1$) differentially expressed by the Empirical Bayes moderated t -test. **a** Dumbbell plot of the mean log₂ baseline expression for patients with PEPI = 0 and PEPI > 0 for each significant phosphoprotein. **b** Dumbbell plot of the mean log₂ change in expression among patients with PEPI = 0 and PEPI > 0 for each significant phosphoprotein.

a Baseline: PEPI=0 vs PEPI>0 RPPA Analysis



b Change with Treatment: PEPI=0 vs PEPI>0



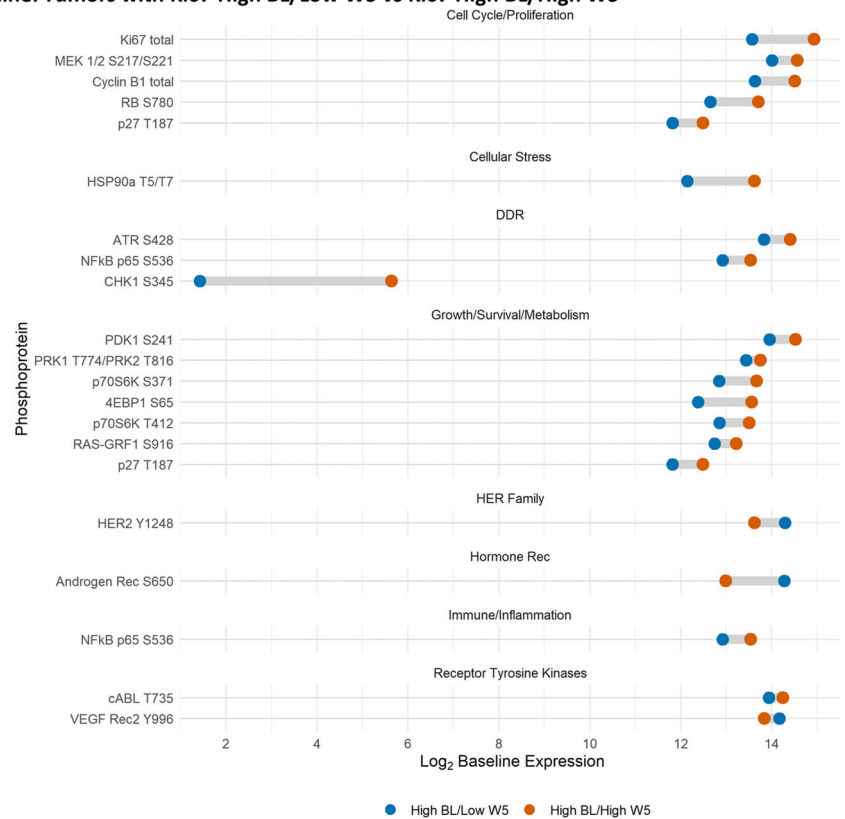
BioSpyder tumor gene expression assay

To identify changes in gene expression following treatment and differences between arms, tempo-seq (Biospyder) was performed using RNA from BL and W5 tissue (Supplementary Data 1 and 2), followed by differential expression analysis and GSEA (Supplementary Data 3 and 4). As would be expected since both arms contained Fulv and both

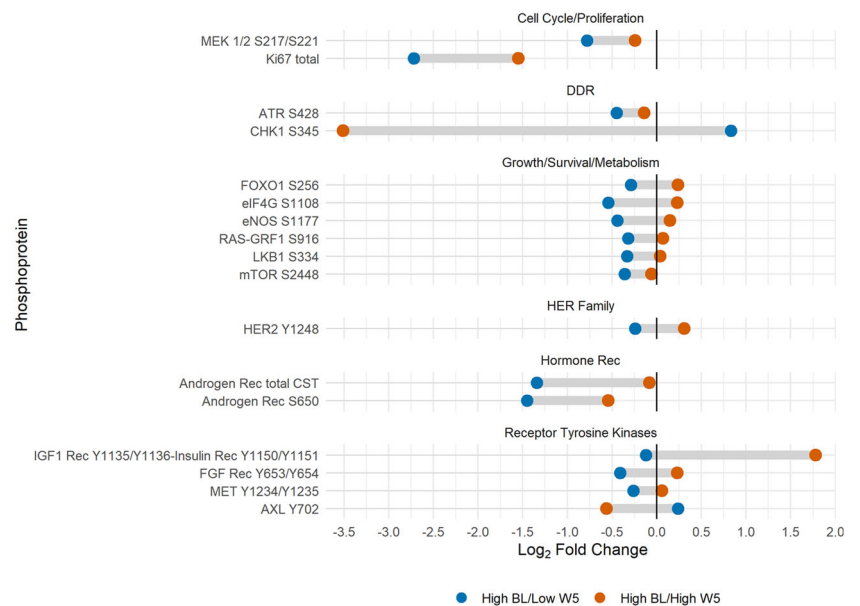
reduced Ki67, changes such as the reduction in estrogen response and cell division gene sets and an increase of adaptive and humoral immune response were significant in both arms (Fig. 6). Interestingly, neither arm showed significant alteration in genes involved in response to androgen signature (largely curated from prostate cancer datasets). However, the Combo arm uniquely increased expression of several

Fig. 4 | RPPA by Ki67 response. RPPA was performed on laser-captured, fresh frozen tumor from the baseline (BL) and week 5 (W5) biopsies. To identify phosphoproteins differentially expressed at BL between tumors that responded to treatment, the samples were split into two groups for comparison: High BL/Low W5, defined as Ki67 > 10% at BL, but ≤10% at W5; versus High BL/High W5, defined as Ki67 > 10% at baseline and >10% remaining at W5. Blue represents High BL/Low W5 (*N* = 13), and orange represents High BL/High W5 (*N* = 9). Presented phosphoproteins were significantly (*p* < 0.1) differentially expressed at the respective time points by the Empirical Bayes moderated *t*-test. **a** Dumbbell plot of the mean log₂ baseline expression for patients with High BL/Low W5 and High BL/High W5 for each significant phosphoprotein. **b** Dumbbell plot of the mean log₂ fold change in expression with treatment (W5–BL) by Ki67 for each phosphoprotein.

a Baseline: Tumors with Ki67 High BL/Low W5 vs Ki67 High BL/High W5



b Change with treatment: Ki67 High BL/Low W5 vs Ki67 High BL/High W5



immune-related genes (e.g., TRIM22, C2, and GNLY) and gene sets related to interferon gamma, complement, inflammation, antigen processing, and B and T cell activation were enriched only in the Combo arm (Fig. 6 and Supplementary Fig. 12).

Multispectral imaging of tumor-associated immune cells

The percentage of total macrophages (CD68+) and myeloid-derived suppressor cells (MDSCs; CD14+, HLADR-, and CD68-) were compared across arms (Fulv, Combo) and time (BL, W5). Macrophages (decreased 0.5

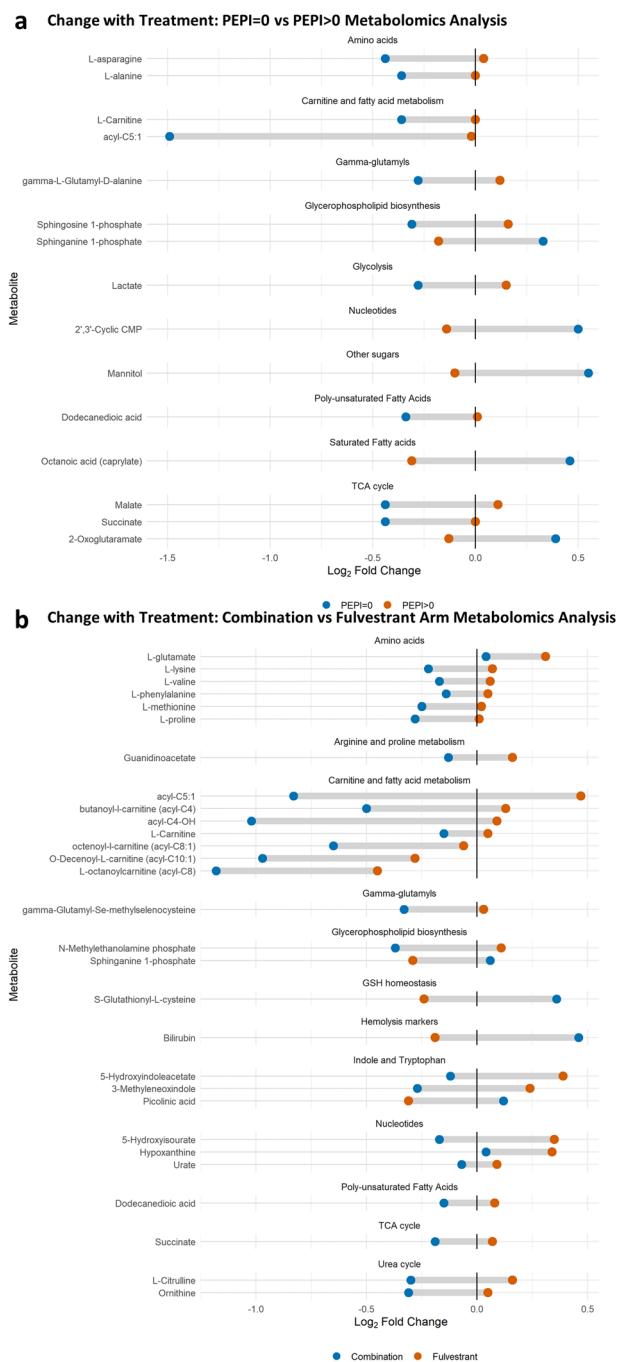


Fig. 5 | Metabolomics change with treatment by PEPI score and Arm. **a** Dumbbell plot of the mean log₂ fold change in expression with treatment (W5–BL) by PEPI score (blue: PEPI = 0 (N = 9), orange: PEPI > 0 (N = 41)) and metabolite. Presented metabolites were significantly ($p < 0.1$) differently expressed with treatment by the eBayes moderated t -test. **b** Dumbbell plot by arm (blue: Combination (N = 29), orange: Fulvestrant (N = 21)).

log₂ units, $p = 0.009$) and MDSCs (decreased 0.1 log₂ units, $p = 0.003$) were significantly reduced by treatment in the paired comparison between BL and W5 only in the Combo arm and were not significantly altered in the Fulv arm (CD68 decreased 0.2 log₂ units, $p = 0.26$; MDSC decreased 0.1 log₂ units, $p = 0.17$) (Fig. 7).

Discussion

The role of AR in ER+ BC has been controversial. Some preclinical modeling suggested that AR agonism might inhibit ER+ BC¹¹; however, this was

predominantly in model systems that had intact ER signaling. Preclinical studies from our group and others showed that AR agonism stimulated ER + BC in the absence of estrogen/ ER signaling, and AR antagonists decreased proliferation^{4,5,12,13}. In the metastatic setting, acquired *ESR1* mutations in aromatase inhibitor treated disease had elevated AR compared to the primary tumor and non-*ESR1* mutated metastases^{14,15}. In the present trial, in patients with primary ER+ BC, AR inhibition with Fulv plus E demonstrated increased tumor histologic response compared to Fulv alone. Specifically, PEPI = 0 was achieved more frequently on the Combo arm (8/33) than the Fulv arm (2/26), although this difference ($p = 0.16$) did not meet the pre-specified ($p < 0.08$) threshold for statistical significance. Importantly, there were no cases in which AR inhibition stimulated the growth of ER+ BC when given together with ER inhibition (as measured by PEPI score or Ki67 response). In fact, no tumors in the Combo arm showed an increase in Ki67 with treatment, but 3 in the Fulv-only arm exhibited increased Ki67. Only one patient that had a T3 tumor at the time of diagnosis achieved PEPI = 0 and this was on the Combo arm and none of the PEPI = 0 patients were node-positive (Table 1).

A major strength of this study was the ability to analyze effects on tumor tissue and plasma using each patient as her own control (via serial specimens). However, even with a randomized design, this trial had limitations, including small patient number and limited number of validated clinical outcome measures. While established by studies conducted by Matthew Ellis and colleagues¹⁶, PEPI score is not optimal as a measure of endocrine therapy sensitivity even with the use of the modified version that excluded ER Allred scoring (due to the use of fulvestrant). As has been observed in the ALTERNATE trial, achievement of PEPI score 0 is rare in patients starting with T3 tumors or nodal involvement as the histologic response to shorter-term exposure to endocrine therapy is more modest. The PEPI score 0 for our control arm (Fulv alone) was significantly lower than that observed in the ALTERNATE trial. This may be in part related to patient selection (over 50% N+) and shorter duration of preoperative therapy. In addition, since Ki67 suppression was not measured for clinical decision, a failure to suppress did not lead to early cessation of endocrine therapy in favor of chemotherapy. Similarly, Ki67 has been used in many trials as a measure of proliferation reduction and clinical response but is not completely reliable due to variations in measurement techniques and quantification¹⁷. Nonetheless, there was a high level of agreement between Ki67 as measured by IHC or by RPPA, improving confidence in the Ki67 component of the PEPI score (Supplementary Discussion 1). Clinical follow-up to determine 5-year disease-free survival is ongoing, although outcome may be affected by post-operative therapy, which was not mandated by this protocol. The choice of 4 months duration of neoadjuvant endocrine therapy was made in 2013, prior to larger trials suggesting that a longer duration of preoperative therapy, such as 6 months, might result in greater histologic/clinical response. Exploratory analyses were hypothesis-generating but limited by small sample size. Therefore, further confirmatory clinical trials are currently being designed.

Similar to our trial using Fulv plus E in the metastatic ER+ BC setting⁹, mTOR pathway activation was greater at BL in tumors with poor histologic response to treatment, suggesting that certain primary tumors may have receptor kinase activation (such as HER2 or activating mutations in the AKT/PI3K/mTOR pathway) that may impart resistance to endocrine therapy. This suggests that further study of AR blockade may be fruitful in patients with metastatic BC treated with endocrine therapy plus PI3K/AKT/mTOR inhibition. In contrast, activated EGFR at BL was associated with tumors destined to achieve PEPI = 0. It is interesting to speculate that the activated EGFR is an indicator of AR activity since liganded AR upregulates the EGFR ligand amphiregulin, and this effect was abrogated by E in vitro and in vivo in preclinical models¹⁸.

When comparing BL pretreatment tumor to W5 of therapy, we used two measures of response: PEPI score at time of surgery and Ki67 (High BL/Low W5 (responsive) versus High BL/High W5 (non-responsive)). In our study, 25% of tumors were non-responsive, which is similar to the 30% in

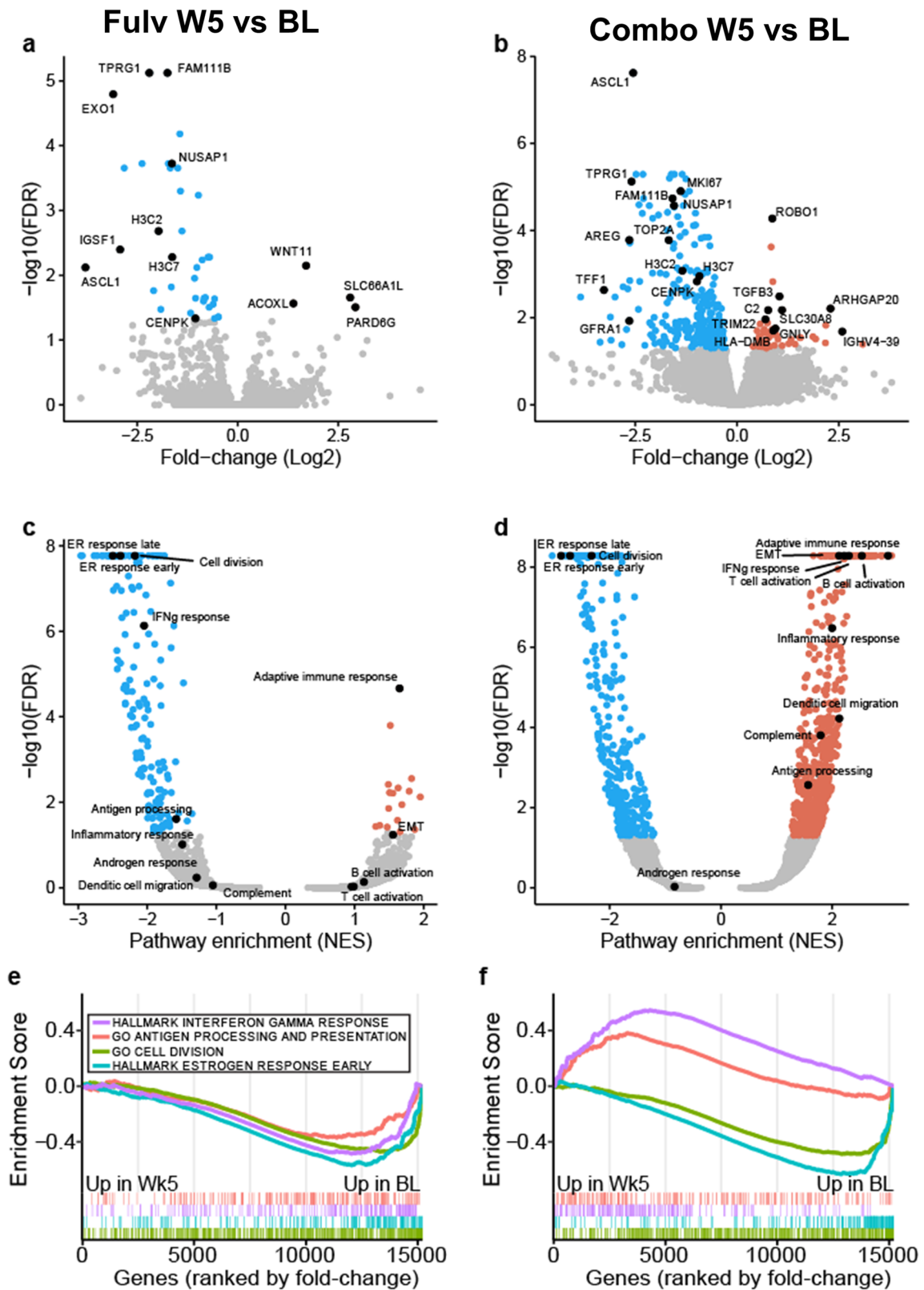


Fig. 6 | Genes and pathways induced by treatment. Paired treated samples were compared to baseline in the Fulvestrant-only arm (left panel; a, c, e) or the combination arm (right; b, d, f). Volcano plots display the differential gene expression results from each comparison (a, b). Select significant genes (FDR < 0.5, red is higher in treatment and blue is higher in baseline) are labeled in black. Volcano plot

displaying GSEA significance and normalized enrichment scores (NES) for each comparison with select pathways labeled (c, d). GSEA enrichment plots displaying select pathways in each comparison (e, f). Below the enrichment score are ticks indicating the ranked positions of genes from each gene set (positive to negative fold change).

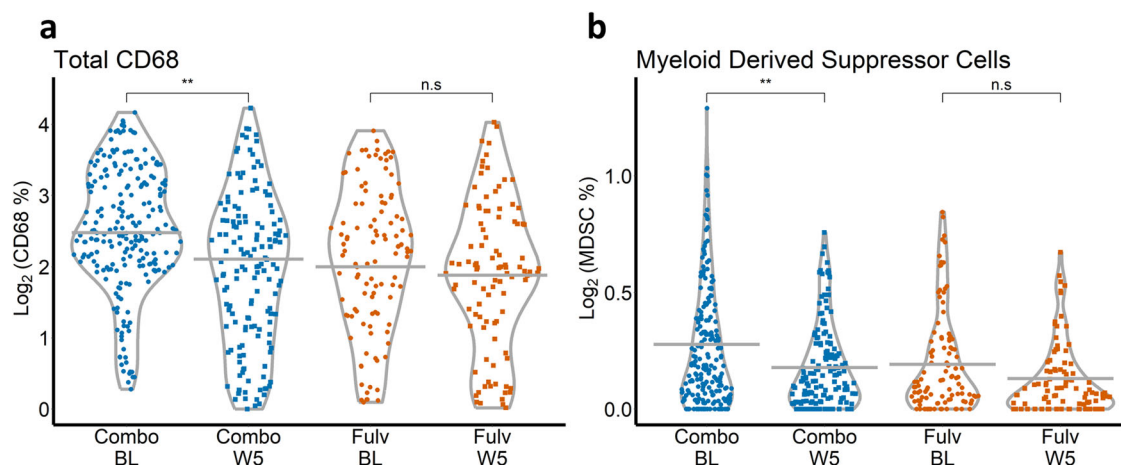


Fig. 7 | Myeloid multiplex. Violin plots are presented for each vectra imaging outcome by treatment arm (Combo, Fulv) and time (BL, W5). Time is on the x-axis, and the log-transformed outcome is on the y-axis. Gray horizontal lines indicate time-specific LMM-predicted averages, and points represent the observed outcome for each of the 576 spectral images collected from 59 patients ($N = 33$ Combo BL, 26

Combo W5, 23 Fulv BL, 25 Fulv W5). P -values were calculated from model contrast statement Z-tests. “n.s.” and “**” indicate non-significance ($p > 0.05$) and $p < 0.01$, respectively. **a** Violin plot of \log_2 CD68. **b** Violin plot of \log_2 myeloid-derived suppressor cells (MDSCs). MDSC expression is defined by the percent of CD14+HLADR-CD68- cells/total cells for this multiplex panel.

ALTERNATE trial¹⁶. By RPPA, total AR was the protein that was most decreased in tumors that achieved PEPI = 0 status compared to PEPI > 0 tumors. In addition, cell cycle, survival and RTK proteins also decreased with treatment in the PEPI = 0 tumors. It is important to note that 8/10 of the PEPI = 0 tumors received the Combo treatment. Overall results were similar when analyzing Ki67 response.

Androgens can have direct effects on immune cells that express AR, as well as indirect effects mediated by AR-regulated immune-modulating factors produced by AR-positive tumor cells. Androgens stimulate immune-suppressive factors¹⁹, some of which, e.g., Chitinase 3-like 1 (CHI3L1, also known as YKL-40 in humans or BRP-39 in mice), support immunosuppressive macrophages, during allergies and cancer²⁰. We previously found that CHI3L1 is regulated by AR in BC¹⁵. In the present study, gene expression data demonstrated that immune stimulating pathways, such as T and B cell activation and antigen processing, were markedly increased by anti-androgen (in the Combo arm). We also observed a significant decrease in macrophages and MDSCs with treatment on the Combo arm (containing anti-androgen) that was not significant in the Fulv arm. In prostate cancer patients with rising prostate-specific antigen (PSA) after definitive therapy, randomized to E for 3 months without androgen deprivation therapy, E was associated with increasing natural killer cells, naïve-T cells, and decreasing MDSC²¹, similar to what we observe in the Combo arm in the present study. In contrast, in AR-independent preclinical models of anti-androgen resistant prostate cancer, E enhanced MDSCs²², perhaps because AR in the tumor cells in the AR-independent models was not regulating factors that attract or enhance MDSCs.

Androgen-activated AR in prostate cancer represses IFN gamma production, and AR blockade with E sensitizes tumor-bearing hosts to checkpoint blockade therapy by directly enhancing CD8 T cell function²⁰. Tumor cell AR may indirectly affect T cell function. In TNBC AR positivity is associated with increased tryptophan catabolism signatures^{23–25}, and the tryptophan catabolite kynurenine expands Tregs and decreases the viability and functionality of cytotoxic T cells^{26–28}. In the present study, the plasma of patients treated on the Combo arm showed evidence of reduced kynurenine pathway catabolites (lower picolinic acid levels), while tryptophan metabolism through indoles was increased, suggesting a possible decrease in immune suppression. This effect was not observed in the Fulv arm. The reduction in tryptophan catabolism, combined with the observed decrease tumor-associated macrophages and MDSCs in the Combo arm, suggests that AR blockade may modulate the tumor immune microenvironment (TIME) in BC (as it does in prostate cancer), and perhaps create a systemic anti-cancer

mode. ER+ BC is the least immunogenic of the BC subtypes²⁹, is not particularly sensitive to anti-PD(L)1 therapies and is thought to require additional immune modulation to make the tumors immunologically active. Therefore, it is possible that further studies evaluating the immune status of ER+ BC with ER plus AR inhibition could lead to trials using immunotherapy to treat ER+ BC. One trial that would further clarify the role of AR inhibition could be a 2nd line trial in luminal BC that combines fulvestrant or oral SERD with PI3K/AKT/mTOR inhibition (considering the observation that mTOR activation appears to be associated with endocrine resistance³) with or without AR blockade, with evaluation of tumor immune microenvironment. A second example would be a 6-month preoperative trial of anti-estrogen therapy plus AR blockade with an addition of immune therapy by ~4 weeks later, with biopsies to confirm the immune activation related to AR blockade. These trials are being designed. Based on the expected low toxicity profile of this proposed combination, a cdk4/6 inhibitor could potentially be added.

Patients with primary resistance to endocrine therapy also did not respond well to chemotherapy, as documented in the ALTERNATE trial¹⁶. Thus, endocrine resistance, as manifested by continued proliferation, must be reversed using novel approaches, including mTOR pathway blockade and harnessing the immune system. In summary, this randomized phase II trial of preoperative Fulv with or without E demonstrated that the addition of AR blockade resulted in a four-fold increase in the number of patients whose tumors achieved a PEPI = 0 score at the time of surgery 4 months later. The trial also shows that AR blockade does not have a stimulatory effect on primary ER+ BC, as some preclinical reports¹¹ had suggested. Mechanisms for the higher number of PEPI = 0 in the Combo arm may include blocking the ability of AR to compensate for ER when ER is degraded by Fulv and/or immune activation by anti-androgen (mediated by a decrease in immune-suppressive cells), leading to a better antitumor response.

Methods

Study design and treatments

NCT02955394 (COMIRB 16-1042) was an open-label randomized phase II trial of fulvestrant with or without enzalutamide. Fulvestrant 500 mg IM was administered on day 1, 15, 29, and then every 4 weeks for a total of 4 months. Enzalutamide 160 mg po daily was given concurrently for 4 months for those women assigned to the combination (Fig. 1A). Surgery was anticipated to occur immediately after week 17 upon completion of enzalutamide; however, timing was subject to surgeon and operating suite availability. As

drug supply was limited, enzalutamide could not always be continued until the day prior to surgery as originally planned. Stratification factors were institution, clinical node status (N0,N+), and T-stage (T2,T3/4). Pre- or peri-menopausal women received concurrent ovarian suppression with a gonadotropin-releasing hormone agonist. The study was conducted at the Universities of Colorado and Tennessee and Memorial Sloan Kettering Cancer Center. The study protocol and its amendments were approved by the respective Institutional Review Boards as well as the Department of Defence HRPO committee. All patients provided written informed consent prior to participating in the study. The study was conducted under the principles of the World Medical Association, Declaration of Helsinki, and Good Clinical Practice guidelines of the International Conference on Harmonisation. The study did not require an Investigational New Drug Application. Drug support (enzalutamide) was provided by Astellas and Pfizer as part of this investigator-sponsored research study.

Study population

Eligible patients were women ≥ 18 years of age with adequate organ and bone marrow function and an ECOG performance score (PS) of 2 or less. All had primary breast cancer of at least 2 cm in size ($\geq T2$, N0-2, M0) determined to be ER positive and HER2 negative. Men were excluded due to potential confounding from androgenic stimuli. History of seizures was exclusionary due to the toxicity profile of enzalutamide. Determination of AR expression was not a requirement as it was expected that $\sim 90\%$ of tumors would stain for AR, and the assay has not yet been validated for clinical decision-making. Concomitant medications with substantial pharmacokinetic (PK) interaction with enzalutamide were avoided.

Safety and antitumor assessment

All patients who received at least one dose of enzalutamide were assessed for safety biweekly for the first 4 weeks, then every 4 weeks until 30 days after the last dose of enzalutamide. Safety and tolerability were determined by assessment of adverse events (AEs), physical examinations, ECOG PS, vital signs, and laboratory tests. The severity of abnormal laboratory values and AEs were classified using the National Cancer Institute Common Terminology Criteria for Adverse Events (CTCAE), version 4.03. SAEs were also evaluated by Astellas Pharma Global Development, United States. A monthly teleconference was held amongst the institutional investigators to review patients and adverse events. An institutional Data Safety and Monitoring Committee at the University of Colorado also had oversight for monitoring.

Tissue acquisition

Fresh tumor biopsies (core needle biopsies of the breast) were required at study entry (BL), and after 4 weeks on therapy (when both Fulv and E were likely at steady state concentrations) and these were termed "W5" biopsy. Fresh frozen and fixed tissue was collected at the time of surgery. Lithium-heparin (LiHep) plasma samples were obtained every 4 weeks until surgery and 1 month after surgery. After collection LiHep vacutainers were centrifuged for 20 min ($600 \times g$), separated plasma was transferred to a 15 mL conical tube, centrifuged a second time for 15 min ($1500 \times g$), aliquoted into 500 μ L aliquots, and stored at -80°C until analysis.

Sample size considerations

Simon 2-stage design for combination (experimental) arm was used:

- If ≤ 3 PEPI = 0 in first 22 patients, then terminate
- If ≥ 4 PEPI = 0, increase arm size to 34 patients
- Probability early termination 0.52 with 80% power with type I error rate of 0.08

Concurrent control arm of Fulv alone assumed that a PEPI = 0 score would be achieved in 16% based on literature experience, requiring a sample size of $n = 27$. If the second stage was achieved, 61 patients would be randomized and treated. We anticipated a 10% unevaluable rate.

All statistical analyses were conducted with two-sided tests, and missing observations were removed from the respective analyses. Due to the exploratory nature of biomarker analyses, the type I error rate for all biomarker analyses was not adjusted for multiple testing.

Clinical benefit rate by PEPI score

PEPI score was calculated on the extent of residual tumor, the nodal status, and the Ki67 on the tumor tissue at time of surgery. ER protein was evaluated by IHC but omitted from the PEPI score evaluation due to an expected downregulation of ER with the use of Fulv. Inclusion of ER did not alter the PEPI score.

Demographic and clinical risk factors of progression

To identify the demographic and clinical risk factors of response by PEPI, the univariate relationships between PEPI (PEPI = 0 ($N = 10$), PEPI > 0 ($N = 49$)) and each of the following risk factors with cell sizes of at least 4 were assessed with univariate logistic regression models: age at consent, Lab AR %, BL and W5 Ki67, and histology (Invasive Ductal Carcinoma (IDC) versus Invasive Lobular Carcinoma (ILC)). Profile likelihood confidence intervals and corresponding likelihood ratio test (LRT) p -values were used.

Serial tissue studies

IHC was performed for ER, progesterone receptor (PR), AR, and glucocorticoid receptor (GR), as well as for Ki67 and cleaved caspase 3 as described previously⁹. T -tests were used to compare the Combo and Fulv arms for each IHC outcome and time point. Paired t -tests were used to evaluate within-arm changes over time. The analyses were performed on 59 patients, with data available from 41–55 patients for any given outcome/time.

Reverse-phase protein array (RPPA)

RPPA was performed as described previously⁹. Briefly, epithelial cells were laser capture microdissected from 8 μ m frozen sections of BL and W5 biopsies, and extracted proteins were printed in triplicate spots onto nitrocellulose-coated slides. Slides were probed with primary antibody targeting each of 116 proteins of interest⁹, followed by biotinylated secondary antibody (Vector Laboratories Inc, Burlingame, CA, or DakoCytomation, Carpinteria, CA), tyramide signal amplification (DakoCytomation), and streptavidin-conjugated IRDye 680 (LI-COR, Lincoln, NE). Total protein was measured using Sypro Ruby protein blot staining (Molecular Probes, Eugene, OR). Proteins were imaged with a Tecan PowerScanner (Tecan, Mannedorf, Switzerland) and analyzed with MicroVigene software Version 5.6. (Vigenetech, Carlisle, MA). Results represent negative control-subtracted and total protein normalized relative intensity values for each endpoint within a given patient sample.

To assess differences in phosphoprotein abundance by PEPI response (response: PEPI = 0, non-response: PEPI > 0), a subset of 54 patients with both BL and W5 RPPA data were analyzed. RPPA samples were collected in two batches for 116 phosphoproteins. Phosphoproteins with available data for less than 5 subjects per group were removed from the dataset, and the data were then normalized with the \log_2 transformation. For each of the phosphoproteins, BL abundance in the 45 patients with PEPI > 0 was compared to the 9 patients with PEPI = 0 with moderated t -tests. An empirical Bayes method was employed to shrink each phosphoprotein's sample variance toward a pooled estimate, allowing for powerful and stable inference³⁰. Variance shrinkage was performed separately for each batch. The same analysis was then performed to assess whether the change in expression from BL to W5 of treatment was significantly different across response groups.

Differences in phosphoprotein abundance by Ki67 response were then analogously assessed at BL and with treatment (W5–BL). The 13 tumors with high BL and low W5 Ki67 (High BL/Low W5) were considered responsive compared to the 9 High BL/High W5, where high Ki67 was defined as Ki67 > 10% and low Ki67 was defined as Ki67 $\leq 10\%$.

Finally, differences in phosphoprotein abundance by histology (ILC ($N=10$), IDC ($N=41$)) were similarly assessed at BL and with treatment (W5–BL).

Metabolomics from patient plasma

Plasma metabolomics analyses were performed in a blinded fashion via UHPLC-MS as previously described^{9,31,32}. Data was acquired on a Vanquish UHPLC coupled online to an Orbitrap Exploris 120 mass spectrometer (Thermo Fisher, Bremen, Germany). Samples were randomized and analyzed using a 5 min gradient with 15 μ L injection in each polarity mode as described^{31,32}. Solvents were supplemented with 0.1% formic acid for positive mode runs and 1 mM ammonium acetate for negative mode runs. MS acquisition, data analysis, and elaboration were performed as described^{9,31,32}.

Differences in metabolite expression were then analyzed by PEPI response with treatment. Metabolites were collected in one batch, and observations under the limits of quantification were imputed with half the minimum of non-missing expression levels of the corresponding metabolite³³. The 8 patients missing either BL or W5 data and one patient missing >50% of metabolites at W5 were then removed such that the analysis was performed on 50 patients (9 PEPI = 0, 41 PEPI > 0). The data were log₂-transformed and analyzed analogously to the RPPA data with moderated *t*-tests. Using the same methods, comparisons by arm were then performed ($n = 21$ Fulv, $n = 29$ Combo).

BioSpyder tumor gene expression assay

Tumor areas from formalin-fixed paraffin-embedded tissue biopsies were macrodissected to enrich the samples for tumor content. The TempO-Seq Human Whole Transcriptome kit from BioSpyder was used to lyse and prepare the samples for shipment. BioSpyder Inc. (Carlsbad, CA) prepared the library. Sequencing of the library was done by the Molecular Pathology Section of the Pathology Shared Resource. Raw gene read counts were generated by BioSpyder. Genes with multiple probes were summed to unique genes. Samples with <40% mapping rate were discarded. Lowly expressed genes were discarded by removing those expressed in less than 10 samples or with less than 1 count per million across all samples. The resulting dataset contained 86 samples and 15,199 genes.

Multispectral imaging of tumor-associated immune cells

BL and W5 FFPE biopsies were stained by the University of Colorado Cancer Center Human Immune Monitoring Shared Resource (HIMSR) using the following primary antibodies: CD14 (SP192, Abcam, Waltham, MA), CD68 (KP1, Dakocytomation, Carpinteria, CA), CD80 (B7-1, R&D Systems, Minneapolis, MN), CD163 (10D6, Abcam), CD209 (C209/1781, Abcam), HLADR (CR3/43, Abcam), PD-L1 (E1L3N(R), Cell Signaling Technology, Danvers MA), and pan-cytokeratin (AE1/AE3, Dakocytomation), and were detected with Opal TSA technology (Akoya Biosciences, Marlborough, MA) using a Leica Bond-III autostainer (Deer Park, IL). Slides were scanned using a Vectra Polaris Quantitative Pathology Imaging System (Akoya Biosciences), and regions that contained tumor were selected for analysis. There were 576 multispectral images collected from 59 patients ($N = 33$ Combo BL, 26 Combo W5, 23 Fulv BL, 25 Fulv W5). First, multispectral images were unmixed, and tissue and cellular compartments were segmented before cells were assigned phenotypes using inForm software, and quantitation of the phenotypes was performed using PhenoptrReports (Akoya Biosciences).

The association between the percentage of Total CD68 cells, treatment arm, and time was first examined with a cell means linear mixed model (LMM) of arm-time group (Combo BL, Fulv BL, Combo W5, Fulv W5) on the log of the percentage of total CD68 cells. The log-transformation was chosen based on visual diagnostics to improve model fit. A random intercept for observation time nested within patients was included. Contrast statements were then used for arm-time group comparisons. The same

analysis was then performed with the myeloid-derived suppressor cells (MDSCs), defined as CD14+, HLADR–, and CD68–, as the outcome of interest (Fig. 7).

Additional analyses

Additional exploratory comparisons were performed but are not presented in this paper due to space constraints and non-significance. The associations between all demographic and clinical risk factors of response were explored univariately with alternative definitions of response: change in Ki67 (Response: High BL/Low W5, Non-Response: High BL/High W5) and W5 Ki67 (Response: $\leq 10\%$, Non-Response: $>10\%$). For RPPA, the following comparisons were made: treatment arms (Fulv, Combo), and an alternative Ki67 definition (Low W5, High W5, regardless of BL). Ki67 comparisons were also descriptively stratified by arm. Finally, metabolomics analyses compared PEPI (PEPI = 0, PEPI > 0) at BL.

Statistical software

All analyses were performed in R version 4.0.4 or later³⁴. Differential expression was calculated with the limma R package³⁵. Gene set enrichment analysis was performed on the fold-changes of each comparison using the clusterProfiler and fgsea R packages^{36,37} with the Hallmarks and Gene Ontology Biological Processes gene set collections from the Molecular Signatures Database³⁸. Data was visualized using the R packages ggplot2³⁹, ggrepel⁴⁰, and plotgardener⁴¹.

Data availability

BioSpyder data is deposited in GEO accession number GSE271080. The metabolomics data presented in this study is available at the NIH Common Fund's National Metabolomics Data Repository (NMDR) website, the Metabolomics Workbench, <https://www.metabolomicsworkbench.org>, where it has been assigned Study ID ST003315. The data can be accessed directly via its Project <https://doi.org/10.21228/M82Z4P>.

Code availability

Data cleaning and analyses were performed in R version 4.0.4 or later, with additional packages as described in the “Statistical software” subsection of the “Methods.” Analyses were also performed with Bioconductor. Code generated to analyze laboratory datasets free of protected health information is available upon reasonable request to the corresponding author.

Received: 19 March 2024; Accepted: 22 September 2024;

Published online: 06 October 2024

References

- Collins, L. C. et al. Androgen receptor expression in breast cancer in relation to molecular phenotype: results from the Nurses' Health Study. *Mod. Pathol.* **24**, 924–931 (2011).
- Ricciardelli, C. et al. The magnitude of androgen receptor positivity in breast cancer is critical for reliable prediction of disease outcome. *Clin. Cancer Res.* **24**, 2328–2341 (2018).
- Cao, L. et al. A high AR:ER α or PDEF:ER α ratio predicts a sub-optimal response to tamoxifen therapy in ER α -positive breast cancer. *Cancer Chemother. Pharmacol.* **84**, 609–620 (2019).
- Cochrane, D. R. et al. Role of the androgen receptor in breast cancer and preclinical analysis of enzalutamide. *Breast Cancer Res.* **16**, R7 (2014).
- D'Amato, N. C. et al. Cooperative dynamics of AR and ER activity in breast cancer. *Mol. Cancer Res.* **14**, 1054–1067 (2016).
- Rangel, N. et al. AR/ER ratio correlates with expression of proliferation markers and with distinct subset of breast tumors. *Cells* **9**, 1064 (2020).
- Rangel, N. et al. The role of the AR/ER ratio in ER-positive breast cancer patients. *Endocr. Relat. Cancer* **25**, 163–172 (2018).

8. Schwartzberg, L. S. et al. A phase I/II study of enzalutamide alone and in combination with endocrine therapies in women with advanced breast cancer. *Clin. Cancer Res.* **23**, 4046–4054 (2017).
9. Elias, A. D. et al. Phase II trial of fulvestrant plus enzalutamide in ER+/HER2- advanced breast cancer. *NPJ Breast Cancer* **9**, 41 (2023).
10. Palmieri, C. et al. Activity and safety of enobosarm, a novel, oral, selective androgen receptor modulator, in androgen receptor-positive, oestrogen receptor-positive, and HER2-negative advanced breast cancer (Study G200802): a randomised, open-label, multicentre, multinational, parallel design, phase 2 trial. *Lancet Oncol.* **25**, 317–325 (2024).
11. Hickey, T. E. et al. The androgen receptor is a tumor suppressor in estrogen receptor-positive breast cancer. *Nat. Med.* **27**, 310–320 (2021).
12. Ciuppek, A. et al. Androgen receptor promotes tamoxifen agonist activity by activation of EGFR in ER α -positive breast cancer. *Breast Cancer Res. Treat.* **154**, 225–237 (2015).
13. De Amicis, F. et al. Androgen receptor overexpression induces tamoxifen resistance in human breast cancer cells. *Breast Cancer Res. Treat.* **121**, 1–11 (2010).
14. Gu, G. et al. Hormonal modulation of ESR1 mutant metastasis. *Oncogene* **40**, 997–1011 (2021).
15. Williams, M. M. et al. Steroid hormone receptor and infiltrating immune cell status reveals therapeutic vulnerabilities of ESR1-mutant breast cancer. *Cancer Res.* **81**, 732–746 (2021).
16. Ma, C. X. et al. Endocrine-sensitive disease rate in postmenopausal patients with estrogen receptor-rich/ERBB2-negative breast cancer receiving neoadjuvant anastrozole, fulvestrant, or their combination: a phase 3 randomized clinical trial. *JAMA Oncol.* **10**, 362–371 (2024).
17. Ellis, M. J. et al. Ki67 proliferation index as a tool for chemotherapy decisions during and after neoadjuvant aromatase inhibitor treatment of breast cancer: results from the American College of Surgeons Oncology Group Z1031 Trial (Alliance). *J. Clin. Oncol.* **35**, 1061–1069 (2017).
18. Barton, V. N. et al. Multiple molecular subtypes of triple-negative breast cancer critically rely on androgen receptor and respond to enzalutamide in vivo. *Mol. Cancer Ther.* **14**, 769–778 (2015).
19. Hanamura, T. et al. Secreted indicators of androgen receptor activity in breast cancer pre-clinical models. *Breast Cancer Res.* **23**, 102 (2021).
20. Guan, X. et al. Androgen receptor activity in T cells limits checkpoint blockade efficacy. *Nature* **606**, 791–796 (2022).
21. Madan, R. A. et al. Clinical and immunologic impact of short-course enzalutamide alone and with immunotherapy in non-metastatic castration sensitive prostate cancer. *J. Immunother. Cancer* **9**, e001556 (2021).
22. Consiglio, C. R., Udartseva, O., Ramsey, K. D., Bush, C. & Gollnick, S. O. Enzalutamide, an androgen receptor antagonist, enhances myeloid cell-mediated immune suppression and tumor progression. *Cancer Immunol. Res.* **8**, 1215–1227 (2020).
23. Doane, A. S. et al. An estrogen receptor-negative breast cancer subset characterized by a hormonally regulated transcriptional program and response to androgen. *Oncogene* **25**, 3994–4008 (2006).
24. Farmer, P. et al. Identification of molecular apocrine breast tumours by microarray analysis. *Oncogene* **24**, 4660–4671 (2005).
25. Lehmann, B. D. et al. Identification of human triple-negative breast cancer subtypes and preclinical models for selection of targeted therapies. *J. Clin. Invest.* **121**, 2750–2767 (2011).
26. Opitz, C. A. et al. An endogenous tumour-promoting ligand of the human aryl hydrocarbon receptor. *Nature* **478**, 197–203 (2011).
27. Solvay, M. et al. Tryptophan depletion sensitizes the AHR pathway by increasing AHR expression and GCN2/LAT1-mediated kynurenine uptake, and potentiates induction of regulatory T lymphocytes. *J. Immunother. Cancer* **11**, e006728 (2023).
28. Greene, L. I. et al. A role for tryptophan-2,3-dioxygenase in CD8 T-cell suppression and evidence of tryptophan catabolism in breast cancer patient plasma. *Mol. Cancer Res.* **17**, 131–139 (2019).
29. Stanton, S. E., Adams, S. & Disis, M. L. Variation in the incidence and magnitude of tumor-infiltrating lymphocytes in breast cancer subtypes: a systematic review. *JAMA Oncol.* **2**, 1354–1360 (2016).
30. Smyth, G. K. Linear models and empirical Bayes methods for assessing differential expression in microarray experiments. *Stat. Appl. Genet. Mol. Biol.* **3**, Article3 (2004).
31. Nemkov, T., Hansen, K. C. & D'Alessandro, A. A three-minute method for high-throughput quantitative metabolomics and quantitative tracing experiments of central carbon and nitrogen pathways. *Rapid Commun. Mass Spectrom.* **31**, 663–673 (2017).
32. Reisz, J. A., Zheng, C., D'Alessandro, A. & Nemkov, T. Untargeted and semi-targeted lipid analysis of biological samples using mass spectrometry-based metabolomics. *Methods Mol. Biol.* **1978**, 121–135 (2019).
33. Damodar, S. & Mehta, D. S. Effect of scaling and root planing on gingival crevicular fluid level of YKL-40 acute phase protein in chronic periodontitis patients with or without type 2 diabetes mellitus: a clinico-biochemical study. *J. Indian Soc. Periodontol.* **22**, 40–44 (2018).
34. R Core Team. R: a language and environment for statistical computing (R Foundation, 2023).
35. Ritchie, M. E. et al. limma powers differential expression analyses for RNA-sequencing and microarray studies. *Nucleic Acids Res.* **43**, e47 (2015).
36. Cai, J. et al. Increased levels of CHI3L1 and HA are associated with higher occurrence of liver damage in patients with obstructive sleep apnea. *Front. Med.* **9**, 854570 (2022).
37. Sergushichev, A. A. An algorithm for fast preranked gene set enrichment analysis using cumulative statistic calculation. Preprint at *bioRxiv*. <https://doi.org/10.1101/060012> (2016).
38. YKL-40. *Arerugi* **66**, 1016–1017 (2017).
39. Wickham, H. *ggplot2: Elegant Graphics for Data Analysis* (Springer, 2016).
40. Slowikowski, K. *ggrepel: Automatically Position Non-overlapping Text Labels With 'ggplot2'*, Vol. 2024 (Github, 2024).
41. Kramer, N. E. et al. Plotgardener: cultivating precise multi-panel figures in R. *Bioinformatics* **38**, 2042–2045 (2022).

Acknowledgements

We acknowledge the University of Colorado Cancer Center Support Grant P30CA046934, particularly extensive use of the Pathology Shared Resource (RRID: SCR_021994), Biorepository section services (RRID: SCR_021989), Bioinformatics and Biostatistics Shared Resource (RRID: SCR_021981), Mass Spectrometry Metabolomics Shared Resource (RRID: SCR_021988), as well as the Human Immune Monitoring Shared Resource (RRID:SCR_021985). We also wish to thank our patient advocates on the DOD BCRP Clinical Translational Award for their input: Jane Perlmutter, PhD, MBA, Karen Raines Hunt, PhD, and we honor the memory of the third patient advocate, Vicki Tosher. We are also very grateful to the patients enrolled in NCT02955394 for their participation. Funding comes from the Department of Defense Breast Cancer Research Program Clinical Translational Award BC120183 W81XWH-13-1-0090/91 (A.D.E., J.K.R.).

Author contributions

Conceptualization: A.D.E., J.K.R. Methodology: N.S.S., S.S., K.L.Z., R.I.G., J.D.W., A.G., K.R.J., J.E.S. Funding acquisition: A.D.E., J.K.R. Patient enrollment: G.A.V., M.F., V.F.B., P.K., J.R.D., E.S., A.D.E. Data curation: A.W.S., K.L.Z., D.G., A.G. Formal analysis: A.W.S., A.G., R.I.G., J.D.W., D.G. Data visualization: N.S.S., A.W.S., V.A., A.G. Project administration: T.M. Writing: A.D.E., A.W.S., E.F.P., J.K.R. Review and editing: A.D.E., N.S.S.,

G.A.V., M.F., V.F.B., P.K., J.R.D., E.S., K.R.J., J.E.S., D.G., V.A. Supervision: A.D.E., E.F.P., D.G., J.K.R.

Competing interests

The authors declare no competing interests.

Additional information

Supplementary information The online version contains supplementary material available at <https://doi.org/10.1038/s41523-024-00697-5>.

Correspondence and requests for materials should be addressed to Jennifer K. Richer.

Reprints and permissions information is available at <http://www.nature.com/reprints>

Publisher's note Springer Nature remains neutral with regard to jurisdictional claims in published maps and institutional affiliations.

Open Access This article is licensed under a Creative Commons Attribution-NonCommercial-NoDerivatives 4.0 International License, which permits any non-commercial use, sharing, distribution and reproduction in any medium or format, as long as you give appropriate credit to the original author(s) and the source, provide a link to the Creative Commons licence, and indicate if you modified the licensed material. You do not have permission under this licence to share adapted material derived from this article or parts of it. The images or other third party material in this article are included in the article's Creative Commons licence, unless indicated otherwise in a credit line to the material. If material is not included in the article's Creative Commons licence and your intended use is not permitted by statutory regulation or exceeds the permitted use, you will need to obtain permission directly from the copyright holder. To view a copy of this licence, visit <http://creativecommons.org/licenses/by-nc-nd/4.0/>.

© The Author(s) 2024

¹Department of Medicine/Medical Oncology, University of Colorado, Anschutz Medical Campus, Aurora, Colorado, USA. ²Department of Pediatrics, University of Colorado, Anschutz Medical Campus, Aurora, Colorado, USA. ³University of Colorado Cancer Center, Biostatistics and Bioinformatics Shared Resource, Aurora, Colorado, USA. ⁴Department of Medical Oncology, Memorial Sloan Kettering Cancer Center, New York, New York, USA. ⁵West Cancer Center and Research Institute and Department of Medicine, University of Tennessee Health Sciences Center, Tennessee, USA. ⁶Department of Pathology, University of Colorado, Anschutz Medical Campus, Aurora, Colorado, USA. ⁷University of Colorado Cancer Center, University of Colorado Anschutz Medical Campus, Aurora, Colorado, USA. ⁸Department of Biomedical Informatics, University of Colorado Anschutz Medical Campus, Aurora, Colorado, USA. ⁹Center for Applied Proteomics and Molecular Medicine, George Mason University, Fairfax, Virginia, USA. ¹⁰University of Colorado Cancer Center, Oncology Clinical Research Support Team, Aurora, Colorado, USA. ¹¹Department of Immunology and Microbiology, University of Colorado, Anschutz Medical Campus, Aurora, Colorado, USA. ✉ e-mail: jennifer.richer@cuanschutz.edu